Supplementary data text

1.1 Optimization data analysis and search for optimum formulation

The optimization data analysis was carried out by apt mathematical modeling using multiple linear regression analysis (MLRA) for fitting the experimental data to the second-order polynomial model with added interaction terms. Only the statistically significant coefficients ($p < 0.05$) were considered in framing the polynomial equations, and the model was evaluated by analyzing the p-value, coefficient of correlation (r^2) and predicted residual sum of squares (PRESS). Response surface analysis was carried out employing 2D-contour plots for understanding the relationship among the studied factors with quality attributes of the formulation. The search for optimum formulation was conducted by numerical desirability function, followed by demarcation of the optimized formulation in the overlay plot design space region. Validation of the optimization methodology was conducted by preparing check-point formulations and comparing the predicted responses with the observed ones with the help of linear correlation plots and residual plots. The percent prediction error (or percent bias) was also calculated for ratifying the prognostic ability of the optimization methodology.

1.2 Optimization data analysis and response surface mapping

The polynomial analysis was carried out for developing the second-order quadratic model employing MLRA. The coefficients of the model equations generated for each of the response variables, as per the Eq. (3) revealed excellent goodness of fit of the experimental data to the selected model, as is evident from the high values of r^2 ranging between 0.9940 and 0.9971 ($p < 0.001$ in all the cases), insignificant lack of fit and low values of PRESS.

$$Y = \beta_0 + \beta_1 X_1 + \beta_2 X_2 + \beta_3 X_3 + \beta_4 X_1 X_2 + \beta_5 X_2 X_3 + \beta_6 X_1 X_3 + \beta_7 X_1^2 + \beta_8 X_2^2 + \beta_9 X_3^2 + \beta_{10} X_1^2 X_2 + \beta_{11} X_2^2 X_3 \quad \text{....Eq. (3)}$$

where, Y=response variables, β_0=intercept, β_1 to β_3= coefficients of linear model terms; β_4 to β_6= coefficients of linear interaction terms, β_7 to β_9= coefficients of quadratic terms, β_{10}, β_{11}= coefficients of quadratic interaction terms.

The model coefficients revealed prevalence of interaction among the studied factors on the responses. Analogously, the 2D-contour plots depicted in **supplementary data Figure 1(A-D)** for the response variables *viz.* particle size, zeta potential, encapsulation efficiency and *in vitro* drug release also construed influence of the studied factors on each of them.

As depicted in 2D-contour plots in **supplementary data Figure 1A**, highly significant influence of the amount of Compritol 888, Solutol HS15 and stirring speed was observed on particle size. Increase in the amount of Compritol 888 revealed a sharp increasing trend on particle size, while amount of Solutol HS15 showed a decreasing trend. The stirring speed also showed negative influence on particle size at all the levels of Compritol 888 and Solutol HS15, respectively. Smaller particle size was observed at low levels of Compritol 888, and high levels of Solutol HS15 and stirring speed. As lipid tends to form the matrix structure during formation of NLPs, increase in the amount of lipid prominently affected the size. On the contrary, Solutol HS15 provides surfactant and stabilizer like property at all the levels to reduce the particle size. High stirring speed also provides reduction in particle size owing to generation of high shear forces and vice-versa.

Supplementary data Figure 1B portraying 2D-contour plots for zeta potential revealed a sharp rising trend with increase in the amount of Solutol HS15 at high levels of Compritol 888. However, increasing in the amount of Compritol 888 revealed a curvilinear trend on zeta potential. String speed, on the other hand, showed miniscule influence on zeta potential. Highly significant influence of Solutol HS15 on zeta potential can be explained owing to its nonionic nature, which causes alteration in the charges at the junction of electrical double layer [57].

Supplementary data Figure 1C depicts the contour plots for effect of varying concentrations of Compritol 888, Solutol HS15 and stirring speed on encapsulation efficiency. Amongst these, both Compritol 888 and Solutol HS15 revealed significant influence on the encapsulation efficiency. Higher levels of Compritol 888 exhibited higher encapsulation efficiency owing to lipophilic nature of the prepared complex. Besides, Solutol

HS15 helps in increasing the encapsulation efficiency owing to its solubilization property facilitating higher loading of the complex in the lipid matrix. On the contrary, stirring speed showed moderate influence with a declining trend on encapsulation efficiency. Maximal encapsulation efficiency was observed at intermediate levels of Compritol 888 and stirring speed, at higher levels of Solutol HS15.

The influence of Compritol 888, Solutol HS15 and stirring speed on $T_{90\%}$ is depicted in **supplementary data Figure 1D,** which revealed sharp increase in the values of $T_{90\%}$ with increasing the amount of Compritol 888 and Solutol HS15. Stirring speed, however, revealed no significant influence on $T_{90\%}$. Being lipophilic in nature, Compritol 888 provides slower drug release rate for solubilization of drug molecules into the dissolution medium. Also the Solutol HS15 is responsible for modulating the drug release profile owing to faster entry of the solvent into the lipid matrix.

Supplementary data figures

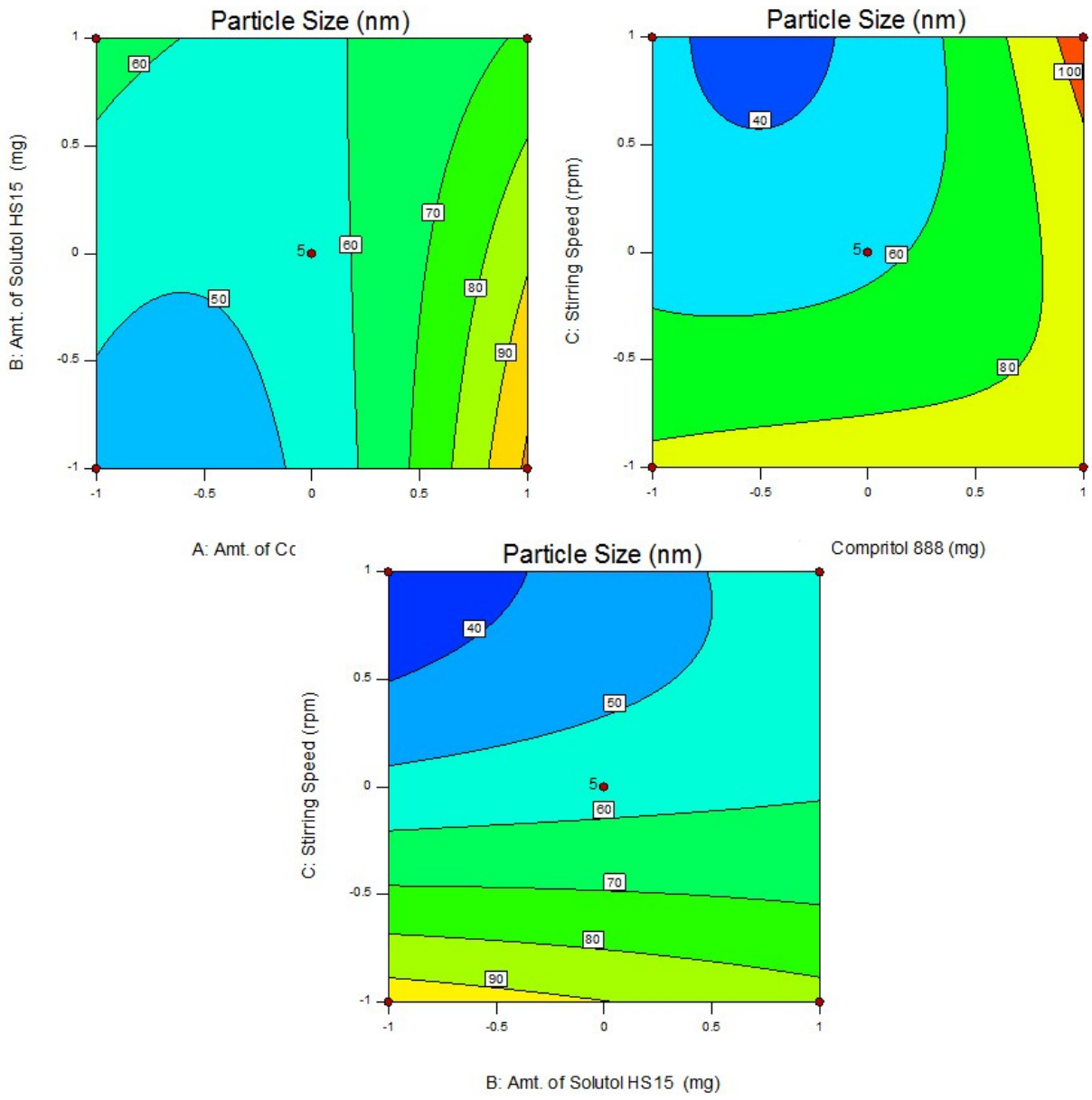

Figure 1A: 2D-contour plots depicting the influence of the amount of Compritol 888, amount of Solutol HS15 and stirring speed on particle size as the response variable

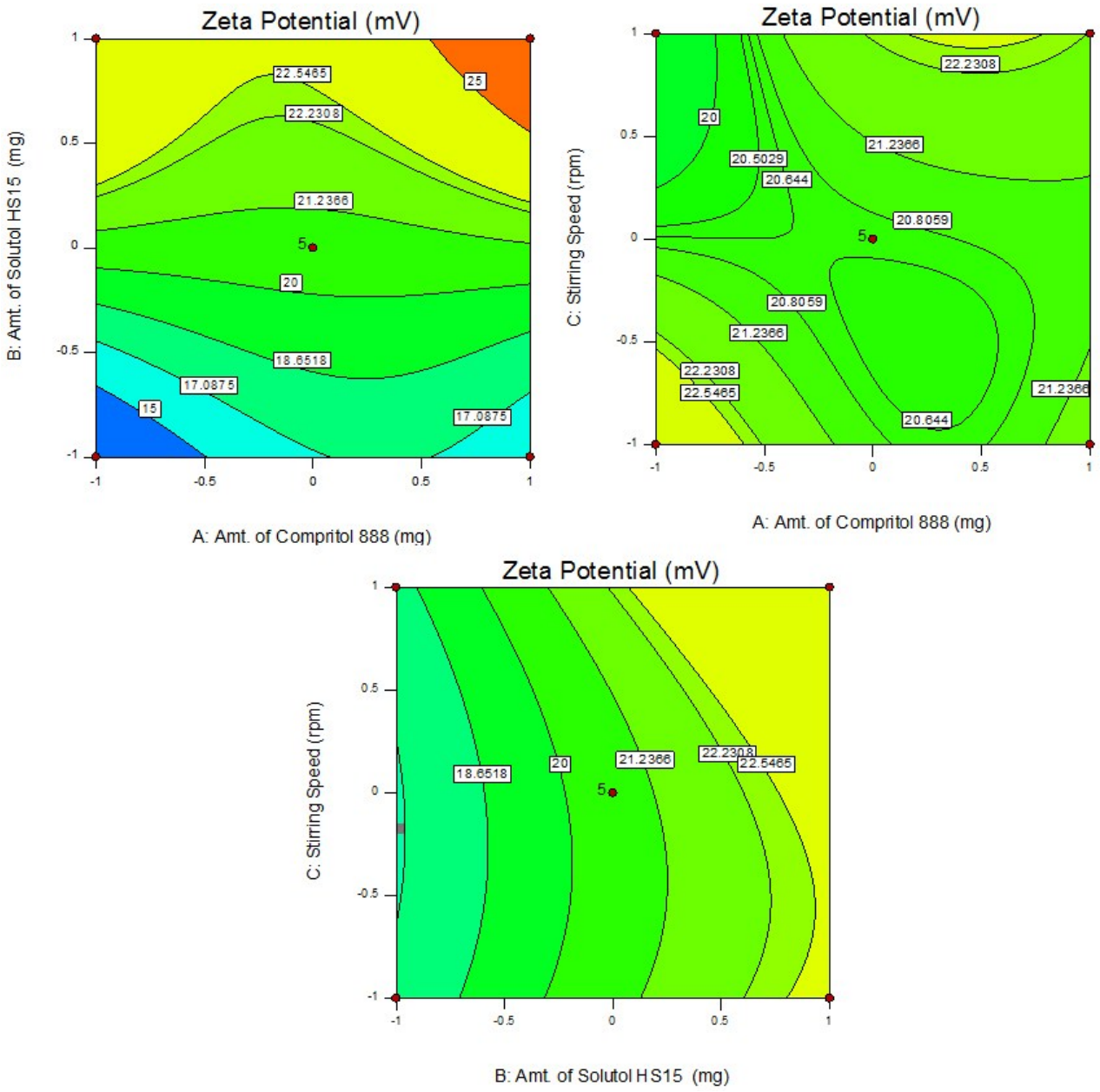

Figure 1B: 2D-contour plots depicting the influence of the amount of Compritol 888, amount of Solutol HS15 and stirring speed on zeta potential as the response variable

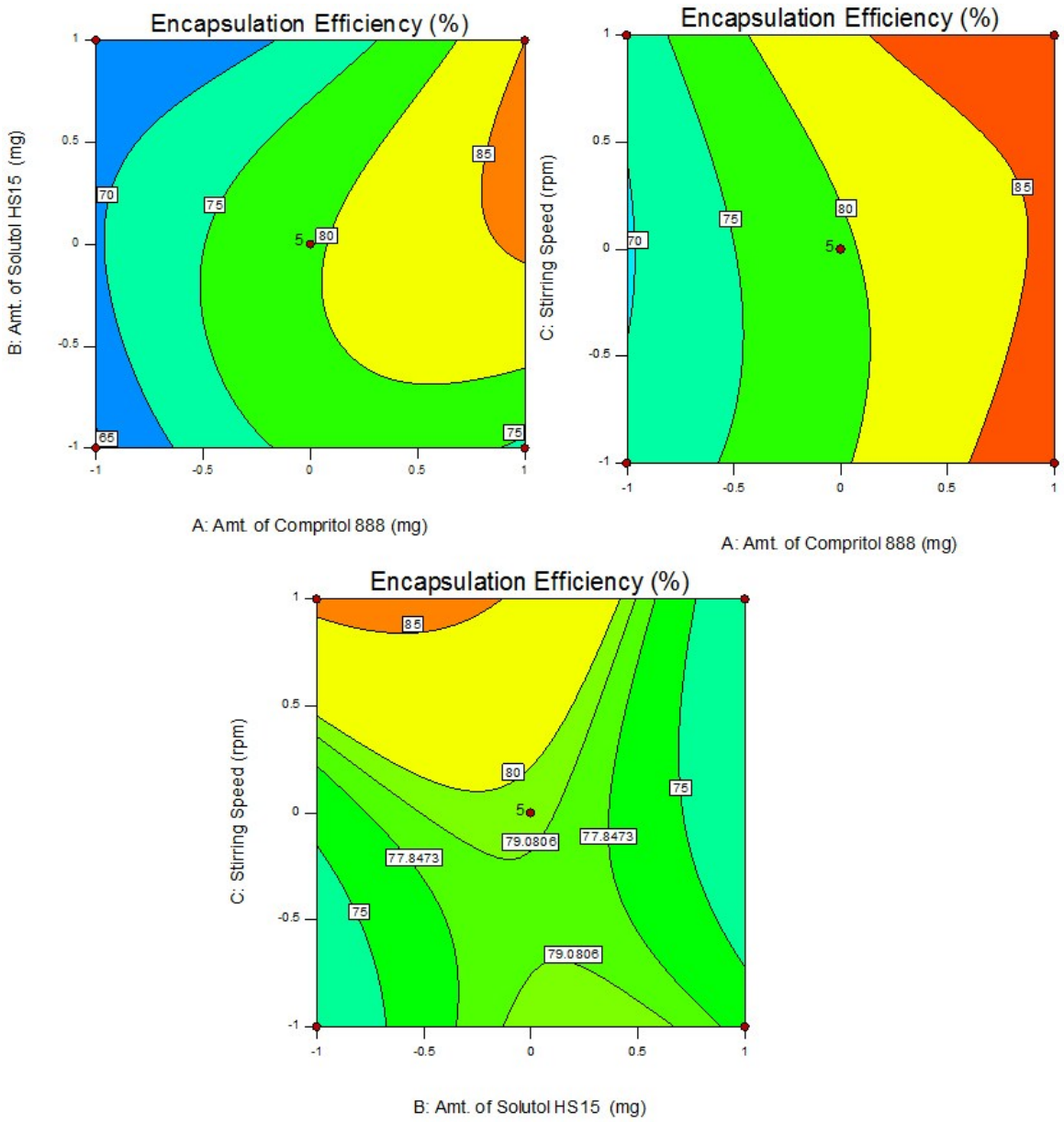

Figure 1C: 2D-contour plots depicting the influence of the amount of Compritol 888, amount of Solutol HS15 and stirring speed on encapsulation efficiency as the response variable

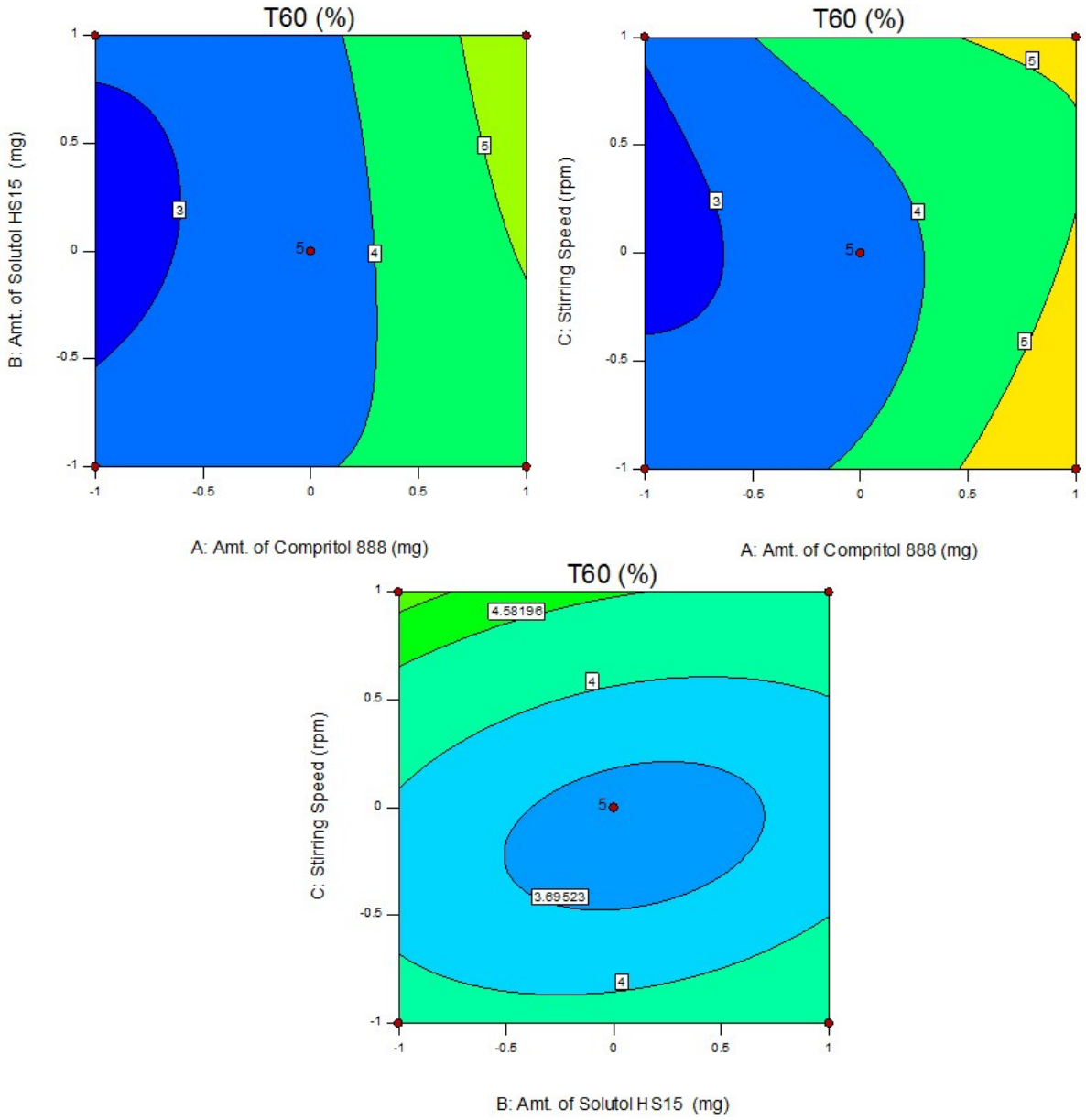

Figure 1D: 2D-contour plots depicting the influence of the amount of Compritol 888, amount of Solutol HS15 and stirring speed on $T_{90\%}$ as the response variable

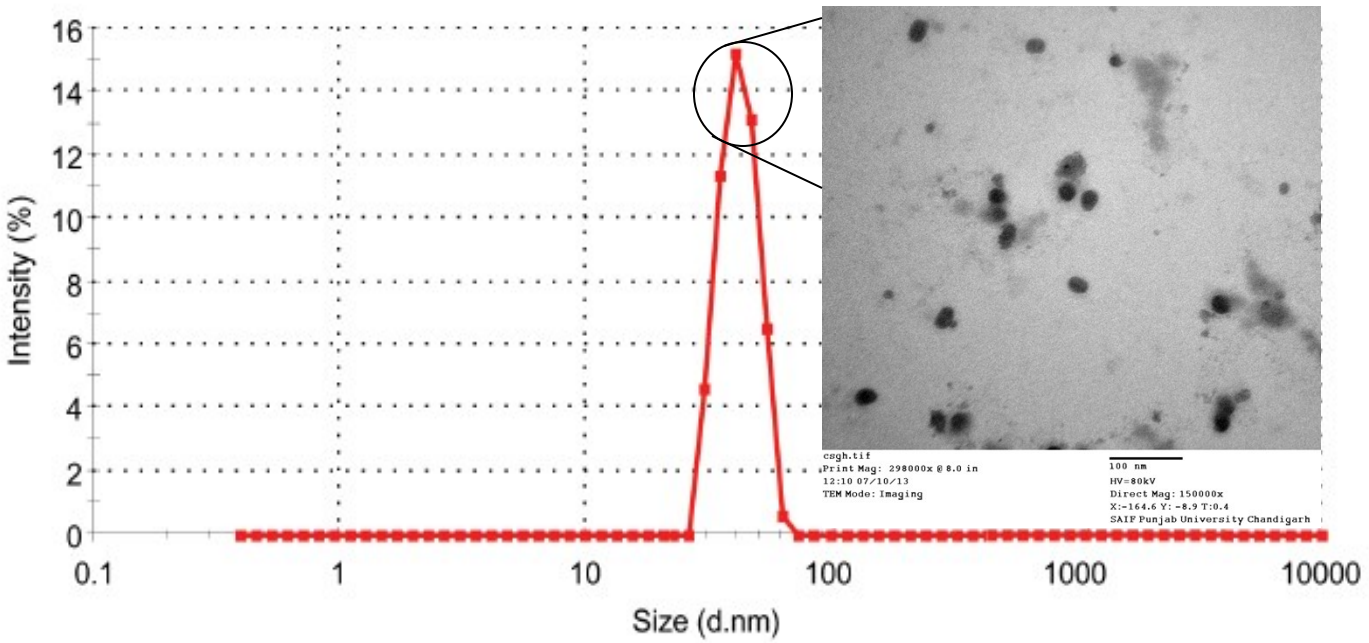

Figure 2: Particle size distribution profile and TEM image of the optimized NLPs

Supplementary data tables

Table 1: Design matrix as per the Box-Behnken design for optimization of NLPs

Trials	Factor X_1	Factor X_2	Factor X_3
F1	1	0	1
F2	-1	0	-1
F3	-1	-1	0
*F4	0	0	0
F5	1	1	0
F6	0	1	1
F7	-1	1	0
F8	1	-1	0
F9	-1	0	1
F10	0	1	-1
F11	0	-1	-1
F12	0	-1	1
F13	1	0	-1
Factors		**Low (-1)**	**High (+1)**
X_1		200	600
X_2		50	100
X_3		1500	3000

*X1: Amt. of Compritol 888 (mg); X2: Amt. of Solutol HS15 (mg); X3: Stirring speed (rpm); *Center point formulation studied for quintuplicate times*

Table 2: Coefficients of polynomial model equations for each response variable and their statistical validity

Coefficient code	Polynomial coefficient values for response variables			
	Particle size (nm)	**Zeta potential (mV)**	**Encapsulation efficiency (%)**	***Time for 90% release ($T_{90\%}$)***
β_0	*56.40*	*20.70*	*79.40*	*3.63*
β_1	*17.25*	*0.20*	*8.00*	*1.18*
β_2	*3.00*	*3.00*	*-2.25*	*-0.078*
β_3	*-23.00*	*0.70*	*2.25*	*0.22*
β_4	*-12.00*	*-0.23*	*2.50*	*0.45*
β_5	*16.25*	*1.60*	*-0.50*	*-0.14*
β_6	*9.00*	*0.35*	*-5.25*	*-0.23*
β_7	*14.93*	*0.19*	*-1.83*	*0.29*
β_8	*-0.32*	*-0.76*	*-5.58*	*0.25*
β_9	*10.92*	*0.91*	*2.43*	*0.77*
β_{10}	*-6.00*	*3.73*	*5.25*	*0.37*
β_{11}	*19.25*	*-2.10*	*-2.75*	*-0.75*
β_{12}	*-1.25*	*1.78*	*-0.50*	*-0.35*
Model P-value	*<0.0001*	*<0.0001*	*<0.0001*	*<0.0001*
r	*0.9971*	*0.9874*	*0.9940*	*0.9944*

Table 3: Values of TC, LDL, HDL and TG levels (mg/dL) in control group and animals subjected to various treatment formulations

Treatment group	Test parameters (mg/dL)	Time (Days)*			
		0	7	14	21
Control	TC	346.48±1.36	325.96±1.11	311.58±3.37	302.51±1.27
	LDL	185.69±0.79	172.89±3.44	166.13±2.01	152.57±2.57
	HDL	19.76±2.47	21.23 ± 2.47	22.76±2.47	24.71±1.06
	TG	213.40±3.22	208.12±1.06	203.34±1.06	198.46±1.06
Pure drug	TC	314.41±1.27	242.77±2.55	184.41±2.41	176.33±2.12
	LDL	178.15±5.02	189.74±3.54	174.76±2.04	143.02±2.11
	HDL	19.44±7.54	24.27±5.49	32.64±1.76	45.04±6.45
	TG	215.27±7.54	195.61±4.55	173.27±6.72	154.27±2.31
Physical mixture	TC	332.22±3.21	196.79±5.69	177.72±3.19	164.49±4.27
	LDL	182.74±5.03	179.21±1.98	162.62±2.59	134.38±1.47
	HDL	18.73±0.69	28.73±0.69	41.22±4.55	47.15±2.41
	TG	227.27±2.04	178.27±1.46	155.45±2.65	137.27±7.54
Complex	TC	352.78±1.55	145.39±2.67	136.26±3.44	124.58±4.14
	LDL	169.20±0.77	156.85±3.54	148.16±3.59	129.12±1.54
	HDL	16.21±0.54	28.33±0.54	48.44±0.54	54.10±3.45
	TG	219.27 ± 7.54	162.76±0.69	149.27±0.89	127.27±7.54
NLPs	TC	346.27±1.42	172.67±1.77	164.11±1.25	115.74±1.45
	LDL	189.72±2.36	138.84±2.69	125.34±3.67	113.85±6.41
	HDL	18.39±3.67	32.27±4.46	56.62±3.97	74.54±4.89
	TG	217.69±5.37	154.46±5.47	122.34±2.44	110.79±2.53

TC: Total cholesterol, TG: Triglyceride, HDL: High-density lipids, LDL: Low-density lipids
**Statistical analysis of different groups performed in comparison to the control group*